Acoustic response of a rigid frame porous medium slab with a periodic set of inclusions

J.-P. Groby [*], A. Wirgin [†] and L. de Ryck[‡] and W. Lauriks [§]

February 1, 2008

Abstract

The acoustic response of a rigid frame porous slab with a periodic set of inclusions is calculated by use of a multipole method. The acoustic properties, in particular the absorption, of such a structure are then derived and studied. Numerical results together with a modal analysis show that the addition of a periodic set of high-contrast inclusions leads to quasi-modes excitation of both the slab and the gratings, and to a large increase of the acoustic absorption of the initial slab, this being partly due to the quasi-modes excitation.

Keywords: absorption of sound, porous materials, periodic inclusions, gratings

1 Introduction

This work was initially motivated by the design problem connected with the determination of the optimal profile of a continuous and/or discontinuous spatial distribution of the material/geometric properties of porous materials for the absorption of sound. The equations that model the acoustic wave propagation in a macroscopically inhomogeneous rigid frame porous medium were derived in [10]. Acoustic properties of porous materials (foam) suffer from a lack of absorption particularly at low frequency. The usual way to solve this problem is by multi-layering [26].

In [24], the authors considered the reflection of a plane acoustic wave by a porous slab that presents a periodic set of pits. The medium is homogenized and its behavior is described in [5]. This leads to a drastic increase of the absorption coeficient at low frequency. In [27] the authors considered the transmission of an acoustic wave through a porous medium in which randomly-arranged metallic rods are imbedded, converted, by a procedure called $ISA\beta$, into an equivalent homogeneous medium which exhibits decreased transmission and increased absorption.

Periodic arrangements of either surface irregularities or volume heterogeneities usually lead to energy entrapment either at the surface or inside the structure, respectively, this being strongly linked to mode excitation, and to an increase of the absorption coefficient (first noticed by Wood [31] and partially explained by Cutler [7]). The particular properties of such structures have been studied in mechanics, with application to composite materials [6, 17, 32], in optics, initially

---
[*]Correspondence to: J.-P. Groby, CMAP, UMR 7641 CNRS/Ecole Polytechnique, 91128 Palaiseau cedex, France
[†]LMA, UPR 7051 CNRS, 31 Chemin Joseph-Aiguier, 13402 Marseille cedex 20, France
[‡]Laboratory of Acoustics and Thermal Physics, Celestijnenlaan 200D, B-3001 Leuven, Belgium
[§]Laboratory of Acoustics and Thermal Physics, Celestijnenlaan 200D, B-3001 Leuven, Belgium

1

motivated by the collection of solar energy [8, 18], with applications to photonic crystals [19, 33], in electromagnetics, with application to so-called left-handed materials [28], in geophysics, for the study of the "city-site" effect [3, 14]. The properties of such structures are now studied to create band-gaps for elastic or acoustic waves (phononic crystals [22, 23, 30]), but have only recently been used for the design of sound absorbing or porous materials [9, 21, 25].

Herein, we study the influence on the acoustic absorption of the introduction of a periodic set of fluid-like circular cylinders into a macroscopically-homogeneous porous slab (the porosity being homogenized in the equivalent fluid model).

2   Formulation of the problem

Both the incident plane acoustic wave and the slab are assumed to be invariant with respect to the Cartesian coordinate x_3. A sagittal x_1-x_2 plane view of the 2D scattering problem is given in Fig. 1.
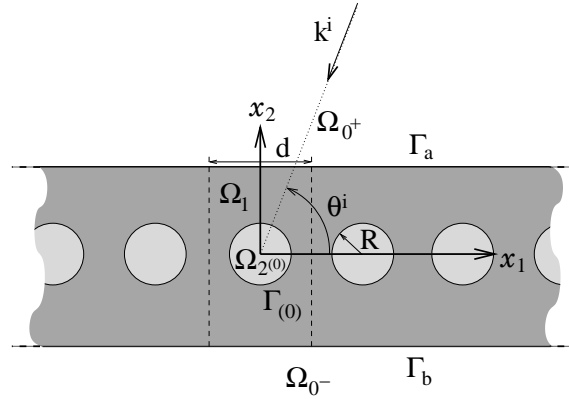

Figure 1: Sagittal plane representation of the configuration of plane wave solicitation of a d-periodic porous slab with fluid-like inclusions (of radius R) within a porous fluid-like slab.

Before the introduction of the cylindrical inclusions, the slab is made of a porous material (e.g., a foam) which is modeled (by homogenization) as a (macroscopically-homogeneous) equivalent fluid M^1. Another equivalent fluid medium M^2 occupies each cylindrical inclusion. In the sagittal plane, the jth cylinder is the circular disk $\Omega_{2(j)}$. The host medium M^0 occupying the two half spaces $\Omega_{0\pm}$ is air. Thus, we are dealing with a macroscopically-inhomogeneous slab, the heterogeneity being periodic in the x_1 direction with period d.

The upper and lower flat, mutually-parallel boundaries of the slab are Γ_a and Γ_b. The x_2 coordinates of these lines are a and b, the thickness h of the slab being $h = a - b$. The circular boundary of $\Omega_{2(j)}$ is $\Gamma_{(j)}$. The center of the $j = 0$ disc is at the origin O of the laboratory system $Ox_1x_2x_3$. The union of Ω_{0+} and Ω_{0-} is denoted by Ω_0.

The wavevector $\mathbf{k}^i$ of the incident plane wave lies in the sagittal plane and the angle of incidence is θ^i measured counterclockwise from the positive x_1 axis.

3   Wave equations

We designate a total pressure and wavenumber by the generic symbols p and k respectively, with $p = p^{0\pm}$, $k = k^0$ in $\Omega_{0\pm}$, $p = p^1$, $k = k^1$ in Ω_1 and $p = p^{2(j)}$, $k = k^2$ in $\Omega_{2(j)}$.

Rather than solving directly for the pressure $p(\mathbf{x}, t)$ (with $\mathbf{x} = (x_1, x_2)$), we prefer to deal with $p(\mathbf{x}, \omega)$, related to $p(\mathbf{x}, t)$ by the Fourier transform:

$$p(\mathbf{x}, t) = \int_{-\infty}^{\infty} p(\mathbf{x}, \omega) e^{-\mathrm{i}\omega t} d\omega \ . \tag{1}$$

Henceforth, we drop the ω in $p(\mathbf{x}, \omega)$ so as to designate the latter by $p(\mathbf{x})$. This function satisfies the Helmholtz equations

$$\left[\triangle + (k^m)^2 \right] p(\mathbf{x}) = 0 \ ; \ \ \mathbf{x} \in \Omega_m \ , \ m = 0^{\pm}, 1, 2 \ . \tag{2}$$

In an equivalent fluid medium [10], the compressibility and density take the form

$$\frac{1}{K_e} = \frac{\gamma P_0}{\phi \left(\gamma - (\gamma - 1) \left(1 + \mathrm{i}\frac{\omega_c}{\mathrm{Pr}^2 \omega} G(\mathrm{Pr}^2 \omega) \right)^{-1} \right)} \ ,$$

$$\rho_e = \frac{\rho_f \alpha_\infty}{\phi} \left(1 + \mathrm{i}\frac{\omega_c}{\omega} F(\omega) \right) \ , \tag{3}$$

where $\omega_c = \dfrac{\sigma\phi}{\rho_f \alpha_\infty}$ is the Biot's frequency cut, γ the specific heat ratio, P_0 the atmospheric pressure, Pr the Prandtl number, ρ_f the density of the fluid in the (interconnected) pores, ϕ the porosity, α_∞ the tortuosity, and σ the flow resistivity. The correction functions $G(\mathrm{Pr}^2 \omega)$ [2], $F(\omega)$ [20] are given by

$$G(\mathrm{Pr}^2 \omega) = \sqrt{1 - \mathrm{i}\frac{\eta \rho_f \alpha_\infty^2}{\sigma^2 \phi^2 \Lambda'^2} \mathrm{Pr}^2 \omega} \ ,$$

$$F(\omega) = \sqrt{1 - \mathrm{i}\frac{\eta \rho_f \alpha_\infty^2}{\sigma^2 \phi^2 \Lambda^2} \omega}. \tag{4}$$

where η is the viscosity of the fluid, Λ' the thermal characteristic length, and Λ the viscous characteristic length.

The incident wave propagates in Ω_{0+} and is expressed by

$$p^i(\mathbf{x}) = A^i \exp[\mathrm{i}(k_1^i x_1 - k_2^i(x_2 - a)] \ , \tag{5}$$

wherein $k_1^i = -k^0 \cos\theta^i$, $k_2^i = k^0 \sin\theta^i$ and $A^i = A^i(\omega)$ is the signal spectrum.

The new feature, with respect to the canonical case considered in [12], is the transverse periodicity of $\cup_{j\in\mathbb{Z}}\Omega_{2(j)}$.

Owing to the plane wave nature of the incident wave, and the periodic nature of $\cup_{j\in\mathbb{Z}}\Omega_{2(j)}$, one can show that the field is quasi-periodic (Floquet theorem), i.e.,

$$p((x_1 + nd, x_2)) = p((x_1, x_2)) e^{\mathrm{i}k_1^i nd} \ ; \ \forall \mathbf{x} \in \mathbb{R}^2 \ ; \ \forall n \in \mathbb{Z} \ . \tag{6}$$

Consequently, it suffices to examine the field in the central cell of the slab which includes the disk $\Omega_{2(0)}$ in order to obtain the fields, via the Floquet relation, in the other cells. Henceforth, we adopt the simplified notation: $\Omega_2 := \Omega_{2(0)}$, $\Gamma := \Gamma_{(0)}$, $p^2 = p^{2^{(0)}}$.

4 Boundary and radiation conditions

Since M^0 and M^1 are fluid-like, the pressure and the normal velocity are continuous across the interfaces Γ_a and Γ_b:

$$p^{0^+}(\mathbf{x}) - p^1(\mathbf{x}) = 0, \ \forall \mathbf{x} \in \Gamma_a \ , \tag{7}$$

$$\left(\rho^0\right)^{-1} \partial_n p^{0^+}(\mathbf{x}) - \left(\rho^1\right)^{-1} \partial_n p^1(\mathbf{x}) = 0, \ \forall \mathbf{x} \in \Gamma_a \ , \tag{8}$$

$$p^{0^-}(\mathbf{x}) - p^1(\mathbf{x}) = 0, \ \forall \mathbf{x} \in \Gamma_b \ , \tag{9}$$

$$\left(\rho^0\right)^{-1} \partial_n p^{0^-}(\mathbf{x}) - \left(\rho^1\right)^{-1} \partial_n p^1(\mathbf{x}) = 0, \ \forall \mathbf{x} \in \Gamma_b \ , \tag{10}$$

wherein $\mathbf{n}$ denotes the generic unit vector normal to a boundary and ∂_n designates the operator $\partial_n = \mathbf{n} \cdot \nabla$.

Since M^1 and M^2 are fluid-like, the pressure and normal velocity are continuous across the interface Γ:

$$p^2(\mathbf{x}) - p^1(\mathbf{x}) = 0, \ \forall \mathbf{x} \in \Gamma \ , \tag{11}$$

$$\left(\rho^2\right)^{-1} \partial_n p^2(\mathbf{x}) - \left(\rho^1\right)^{-1} \partial_n p^1(\mathbf{x}) = 0, \ \forall \mathbf{x} \in \Gamma \ . \tag{12}$$

The uniqueness of the solution to the forward-scattering problem is assured by the radiation conditions :

$$p^{0^+}(\mathbf{x}) - p^i(\mathbf{x}) \sim \ \text{outgoing waves} \ ; \ |\mathbf{x}| \to \infty \ , \ x_2 > a \ , \tag{13}$$

$$p^{0^-}(\mathbf{x}) \sim \ \text{outgoing waves} \ ; \ \forall \, |\mathbf{x}| \to \infty \ , \ x_2 < b \ . \tag{14}$$

5 Field representations

Separation of variables, the radiation conditions, and the Floquet theorem lead to the representations:

$$p^{0^+}(\mathbf{x}) = \sum_{p \in \mathbb{Z}} \left[e^{-\mathrm{i}k_{2p}^0 (x_2 - a)} \delta_{p0} + R_p e^{\mathrm{i}k_{2p}^0 (x_2 - a)} \right] e^{\mathrm{i}k_{1p} x_1}, \ \forall \mathbf{x} \in \Omega_{0^+} \ , \tag{15}$$

$$p^{0^-}(\mathbf{x}) = \sum_{p \in \mathbb{Z}} T_p e^{\mathrm{i}\left(k_{1p} x_1 - k_{2p}^0 (x_2 - b)\right)}, \ \forall \mathbf{x} \in \Omega_{0^-} \ , \tag{16}$$

wherein δ_{p0} is the Kronecker symbol, $k_{1p} = k_1^i + \dfrac{2p\pi}{d}$, $k_{2p}^0 = \sqrt{(k^0)^2 - (k_{1p})^2}$, with $\Re\left(k_{2p}^0\right) \geq 0$ and $\Im\left(k_{2p}^0\right) \geq 0$.

The field in the central inclusion, with $[\mathbf{r} = (r, \theta)]$, takes the form

$$p^2(\mathbf{r}) = \sum_{l \in \mathbb{Z}} C_l J_l\left(k^2 r\right) e^{\mathrm{i}l\theta}, \ \forall (r, \theta) \in \Omega_2 \ , \tag{17}$$

wherein J_l is the l-th order Bessel function.

It is convenient to combine Cartesian coordinates (x_1, x_2) and cylindrical coordinates (r, θ) to write the field representation in Ω_1. The latter takes the form of the sum (by use of the superposition principe) of the diffracted field by the inclusions $p_d^1(\mathbf{x})$ and of the diffracted field in the slab $p_s^1(\mathbf{x})$.

Because of the quasi-periodic aspect of the configuration, the diffracted field in the slab can be written in Cartesian coordinates as:

$$p_s^1(\mathbf{x}) = \sum_{p \in \mathbb{Z}} \left(f_{1p}^- e^{-\mathrm{i} k_{2p}^1 x_2} + f_{1p}^+ e^{\mathrm{i} k_{2p}^1 x_2} \right) e^{\mathrm{i} k_{1p} x_1} \ . \tag{18}$$

We transform Cartesian to polar coordinates by means of:

$$\begin{aligned} x_1 &= r \cos(\theta) \ , \quad k_{1p} = k^1 \cos(\theta_p) \ , \\ x_2 &= r \sin(\theta) \ , \quad k_{2p}^1 = k^1 \sin(\theta_p) \ , \end{aligned} \tag{19}$$

so that

$$p_s^1(\mathbf{r}) = \sum_{p \in \mathbb{Z}} \left(f_{1p}^- e^{\mathrm{i} k^1 r \cos(\theta + \theta_p)} + f_{1p}^+ e^{\mathrm{i} k^1 r \cos(\theta - \theta_p)} \right) \ . \tag{20}$$

Use of the identity

$$e^{\mathrm{i} k^1 r \cos(\theta - \theta_p)} = \sum_{m \in \mathbb{Z}} \mathrm{i}^m J_m(kr) e^{\mathrm{i} m(\theta - \theta_p)} \ , \tag{21}$$

leads to

$$\begin{aligned} p_s^1(\mathbf{r}) &= \sum_{m \in \mathbb{Z}} \sum_{p \in \mathbb{Z}} \mathrm{i}^m \left(f_{1p}^- e^{\mathrm{i} m \theta_p} + f_{1p}^+ e^{-\mathrm{i} \theta_p} \right) e^{\mathrm{i} m \theta} \\ &= \sum_{m \in \mathbb{Z}} \sum_{p \in \mathbb{Z}} \left(f_{1p}^- J_{mp}^- + f_{1p}^+ J_{mp}^+ \right) e^{\mathrm{i} m \theta} \ , \end{aligned} \tag{22}$$

wherein $J_{mp}^- = \mathrm{i}^m e^{\mathrm{i} m \theta_p}$ and $J_{mp}^+ = \mathrm{i}^m e^{-\mathrm{i} m \theta_p}$.

Let us now introduce: i) $(r^j(P), \theta^j(P))$, the polar coordinates of a point P in the system linked to the jth cylinder whose center is at the origin O_j, and ii) (r_l^j, θ_l^j) the polar coordinates of the origin O_j in the polar coordinate system linked to the lth cylinder.

In the general case, the field diffracted by the inclusion appears as the sum of the fields diffracted by all the inclusions:

$$p_d^1(\mathbf{x}) = \sum_{j \in \mathbb{Z}} \sum_{m \in \mathbb{Z}} B^j H_m^{(1)} \left(k^1 r^j \right) e^{\mathrm{i} m \theta^j} \ , \tag{23}$$

wherein $H_m^{(1)}$ is the first-kind Hankel function of order m.

Using Graf's formula [1] for the Hankel function leads to

$$p_d^1(\mathbf{r}) = \sum_{j \in \mathbb{Z} \cap \{0\}} \sum_{m \in \mathbb{Z}} \sum_{q \in \mathbb{Z}} J_m^{(1)} \left(k^1 r \right) e^{\mathrm{i} m \theta} H_{m-q}^{(1)} \left(k^1 r_0^j \right) e^{\mathrm{i}(q-m) \theta_0^j} B_q^j$$

$$+ \sum_{m \in \mathbb{Z}} B^0 H_m^{(1)} \left(k^1 r \right) e^{\mathrm{i} m \theta}, \text{ for } R \le r \le (d - R) \ . \tag{24}$$

In the case of gratings, $r_0^j = j \times d$, $\theta_0^j = \pi$ if $j < 0$ or $\theta_0^j = 0$ if $j \ge 0$, and the quasiperiodicity implies that the multipole expansion coefficients relative to the jth cylinder of the grating are given by $B_m^j = e^{\mathrm{i} k_i^1} B_m^0 = e^{\mathrm{i} k_i^1} B_m$, $\forall m \in \mathbb{Z}$.

The field expansion in the vicinity of the central cylinder then takes the following form (in agreement with [29]):

$$p_d^1(\mathbf{r}) = \sum_{l\in\mathbb{Z}} B_l H_l^{(1)}\left(k^1 r\right) e^{\mathrm{i}l\theta}$$

$$+ \sum_{l\in\mathbb{Z}} J_l\left(k^1 r\right) e^{\mathrm{i}l\theta} \sum_{m\in\mathbb{Z}} S_{l-m} B_m, \text{ for } R \le r \le (d-R) . \quad (25)$$

with $S_l = \sum_{j=1}^{\infty} H_l^{(1)}\left(k^1 jd\right)\left[e^{\mathrm{i}k_1^i jd} + (-1)^l e^{-\mathrm{i}k_1^i jd}\right]$.

To derive an alternative form of (25) in Cartesian coordinates, it is more convenient to start from Green's theorem

$$p_d^1(\mathbf{r}) = \int_\Gamma \left[\frac{\partial p}{\partial n}(\mathbf{r^s})G(\mathbf{r}-\mathbf{r^s}) - \frac{\partial G}{\partial n}(\mathbf{r}-\mathbf{r^s})p(\mathbf{r^s})\right] d\mathbf{r^s} , \quad (26)$$

wherein G is the Green's function

$$G(\mathbf{r}-\mathbf{r^s}) = \frac{i}{2d}\sum_{p\in\mathbb{Z}}\frac{1}{k_{2p}}e^{\mathrm{i}k_{1p}(x_1-x_1^s)+\mathrm{i}k_{2p}|x_2-x_2^s|} , \quad (27)$$

or, with $[\mathbf{r^s} = (r^s, \theta^s)]$ and for $R \le x_2$

$$\begin{aligned} G(\mathbf{r}-\mathbf{r^s}) &= \frac{i}{2d}\sum_{p\in\mathbb{Z}}\frac{1}{k_{2p}}e^{\mathrm{i}k_{1p}x_1+\mathrm{i}k_{2p}x_2}e^{-\mathrm{i}k_{1p}x_1^s-\mathrm{i}k_{2p}x_2^s} \\ &= \frac{i}{2d}\sum_{p\in\mathbb{Z}}\frac{1}{k_{2p}}e^{\mathrm{i}k_{1p}x_1+\mathrm{i}k_{2p}x_2}e^{-\mathrm{i}r^s\cos(\theta^s-\theta_p)} , \end{aligned} \quad (28)$$

so that with the help of identity (21), we are led to

$$p_d^1(\mathbf{x}) = \frac{i}{2d}\sum_{p\in\mathbb{Z}}\frac{1}{k_{2p}}e^{\mathrm{i}k_{1p}x_1+\mathrm{i}k_{2p}x_2} \times \mathcal{I} , \quad (29)$$

with

$$\begin{aligned} \mathcal{I} &= -\int_0^{2\pi} kR d\theta \sum_{m\in\mathbb{Z}}(-\mathrm{i})^m J_m\left(kR\right)e^{\mathrm{i}m(\theta_p-\theta)}\sum_{l\in\mathbb{Z}}\left[B_l\dot{H}_l^{kR} + \sum_{n\in\mathbb{Z}}S_{l-n}B_n\dot{J}_l(kR)\right]e^{\mathrm{i}l\theta} \\ &\quad + \int_0^{2\pi} kR d\theta \sum_{m\in\mathbb{Z}}(-\mathrm{i})^m \dot{J}_m\left(kR\right)e^{\mathrm{i}m(\theta_p-\theta)}\sum_{l\in\mathbb{Z}}\left[B_l H_l^{kR} + \sum_{n\in\mathbb{Z}}S_{l-n}B_n J_l(kR)\right]e^{\mathrm{i}l\theta} \\ &= \frac{-\mathrm{i}\pi}{d}\sum_{m\in\mathbb{Z}}(-\mathrm{i})^m e^{\mathrm{i}m\theta_p}kR\left[J_m(kR)\dot{H}_m^{(1)}(kR) - H_m^{(1)}(kR)\dot{J}_m(kR)\right]B_m \\ &= \frac{2}{d}\sum_{m\in\mathbb{Z}}(-\mathrm{i}^m)e^{\mathrm{i}m\theta_p}B_m , \end{aligned} \quad (30)$$

wherein we have used the fact that $J_{-m}(kR)\dot{H}_m^{(1)}(kR) - H_m^{(1)}(kR)\dot{J}_{-m}(kR) = \dfrac{2\mathrm{i}}{\pi kR}$.

6

Proceeding in the same way for $-R \geq x_2$ gives:

$$p_d^1(\mathbf{x}) = \frac{i}{2d} \sum_{p \in \mathbb{Z}} \frac{1}{k_{2p}} e^{\mathrm{i}k_{1p}x_1 - \mathrm{i}k_{2p}x_2} \times \mathcal{I} , \qquad (31)$$

wherein

$$
\begin{aligned}
\mathcal{I} &= -\int_0^{2\pi} kRd\theta \sum_{m \in \mathbb{Z}} (-\mathrm{i})^m J_m(kR) e^{\mathrm{i}m(\theta_p + \theta)} \sum_{l \in \mathbb{Z}} \left[B_l \dot{H}_l^{kR} + \sum_{m \in \mathbb{Z}} S_{l-m} B_m \dot{J}_l(kR) \right] e^{\mathrm{i}l\theta} \\
&+ \int_0^{2\pi} kRd\theta \sum_{m \in \mathbb{Z}} (-\mathrm{i})^m \dot{J}_m(kR) e^{\mathrm{i}m(\theta_p + \theta)} \sum_{l \in \mathbb{Z}} \left[B_l H_l^{kR} + \sum_{m \in \mathbb{Z}} S_{l-m} B_m J_l(kR) \right] e^{\mathrm{i}l\theta} \\
&= \frac{-\mathrm{i}\pi}{d} \sum_{m \in \mathbb{Z}} (\mathrm{i})^m e^{-\mathrm{i}m\theta_p} kR \left[J_{-m}(kR) \dot{H}_m^{(1)}(kR) - H_m^{(1)}(kR) \dot{J}_{-m}(kR) \right] B_m \\
&= \frac{2}{d} \sum_{m \in \mathbb{Z}} (-\mathrm{i})^m e^{\mathrm{i}m\theta_p} B_m .
\end{aligned}
\qquad (32)
$$

The field diffracted by the inclusion is expressed in Cartesian coordinates by

$$p_d^1(\mathbf{x}) = \sum_{p \in \mathbb{Z}} \sum_{l \in \mathbb{Z}} K_{pl}^{\pm} B_l e^{\mathrm{i}\left(k_{1p}x_1 \pm k_{2p}^1 x_2\right)} , \qquad (33)$$

where the signs $+$ and $-$ correspond to $x_2 > R$ and $x_2 < R$ respectively, and

$$K_{pm}^+ = \frac{2(-\mathrm{i})^m}{dk_{2p}^1} e^{\mathrm{i}m\theta_p}, \ K_{pm}^- = \frac{2(-\mathrm{i})^m}{dk_{2p}^1} e^{-\mathrm{i}m\theta_p} , \qquad (34)$$

with θ_p such that $k^1 e^{\mathrm{i}\theta_p} = k_{1p} + \mathrm{i}k_{2p}^1$, [4, 29].

6   Application of the continuity conditions

Here we consider only the equations of continuity across the interfaces Γ_a and Γ_b. The continuity conditions across Γ will be treated in section 7.

6.1   Continuity of the pressure field across Γ_a

From (7) we obtain

$$\int_{-\frac{d}{2}}^{\frac{d}{2}} p^{0^+}((x_1, a)) e^{-\mathrm{i}k_{1l}x_1} dx1 - \int_{-\frac{d}{2}}^{\frac{d}{2}} p^1((x_1, a)) e^{-\mathrm{i}k_{1l}x_1} dx_1 = 0, \ \forall l \in \mathbb{Z} . \qquad (35)$$

Introducing the appropriate field representations therein and making use of the orthogonality relation

$$\int_{-\frac{d}{2}}^{\frac{d}{2}} e^{\mathrm{i}(k_{1n} - k_{1l})x_1} dx_1 = d\delta_{nl}, \ \forall (l, n) \in \mathbb{Z}^2 , \qquad (36)$$

gives rise to

$$\delta_{p0} + R_p - f_{1p}^- e^{-\mathrm{i}k_{2p}^1 a} - f_{1p}^+ e^{\mathrm{i}k_{2p}^1 a} - \sum_{l \in \mathbb{Z}} K_{pl}^+ B_l e^{\mathrm{i}k_{2p}^1 a} = 0 . \qquad (37)$$

7

6.2 Continuity of the normal component of the velocity across Γ_a

From (8) we obtain

$$\int_{-\frac{d}{2}}^{\frac{d}{2}} (\rho^0)^{-1} \partial_{x_2} p^{0^+}((x_1,a)) e^{-\mathrm{i}k_{1l}x_1} dx1$$

$$- \int_{-\frac{d}{2}}^{\frac{d}{2}} (\rho^1)^{-1} \partial_{x_2} p^1((x_1,a)) e^{-\mathrm{i}k_{1l}x_1} dx_1 = 0, \ \forall l \in \mathbb{Z} \ . \quad (38)$$

Introducing the appropriate field representation therein, and making use of the orthogonality relation (36), gives rise to

$$- \alpha_p^0 \delta_{p0} + \alpha_p^0 R_p + f_{1p}^- \alpha_p^1 e^{-\mathrm{i}k_{2p}^1 a} - f_{1p}^+ \alpha_p^1 e^{\mathrm{i}k_{2p}^1 a} - \sum_{l \in \mathbb{Z}} K_{pl}^+ B_l \alpha_p^1 e^{\mathrm{i}k_{2p}^1 a} = 0 \ , \quad (39)$$

wherein $\alpha_p^i = \dfrac{k_{2p}^i}{\rho^i}$, $\forall i = 0, 1$.

6.3 Continuity of the pressure field across Γ_b

From (9) we obtain

$$\int_{-\frac{d}{2}}^{\frac{d}{2}} p^{0^-}((x_1,b)) e^{-\mathrm{i}k_{1l}x_1} dx1 - \int_{-\frac{d}{2}}^{\frac{d}{2}} p^1((x_1,b)) e^{-\mathrm{i}k_{1l}x_1} dx_1 = 0, \ \forall l \in \mathbb{Z} \ . \quad (40)$$

Introducing the appropriate field representation therein, and making use of the orthogonality relation (36), gives rise to

$$T_p - f_{1p}^- e^{-\mathrm{i}k_{2p}^1 b} - f_{1p}^+ e^{\mathrm{i}k_{2p}^1 b} - \sum_{l \in \mathbb{Z}} K_{pl}^- B_l e^{\mathrm{i}k_{2p}^1 b} = 0 \ . \quad (41)$$

6.4 Continuity of the normal component of the velocity across Γ_b

From (10) we obtain

$$\int_{-\frac{d}{2}}^{\frac{d}{2}} (\rho^0)^{-1} \partial_{x_2} p^{0^-}((x_1,b)) e^{-\mathrm{i}k_{1l}x_1} dx1$$

$$- \int_{-\frac{d}{2}}^{\frac{d}{2}} (\rho^1)^{-1} \partial_{x_2} p^1((x_1,b)) e^{-\mathrm{i}k_{1l}x_1} dx_1 = 0, \ \forall l \in \mathbb{Z} \ . \quad (42)$$

Introducing the appropriate field representation therein, and making use of the orthogonality relation (36), gives rise to

$$- \alpha_p^0 T_p + f_{1p}^- \alpha_p^1 e^{-\mathrm{i}k_{2p}^1 b} - f_{1p}^+ \alpha_p^1 e^{\mathrm{i}k_{2p}^1 b} + \sum_{l \in \mathbb{Z}} K_{pl}^- B_l \alpha_p^1 e^{\mathrm{i}k_{2p}^1 b} = 0 \ . \quad (43)$$

8

7   Determination of the unknowns

From (36), (39), (41) and (43) we get the expressions of f_{1p}^- and f_{1p}^+ in terms of B_l. Introducing the latter into (18) together with (25) leads to

$$
\begin{aligned}
p^1(\mathbf{x}) = {}& \sum_{l\in\mathbb{Z}} B_l H_l^{(1)}\left(k^1 r\right) e^{\mathrm{i}l\theta} + \sum_{l\in\mathbb{Z}} J_l\left(k^1 r\right) e^{\mathrm{i}l\theta} \sum_{m\in\mathbb{Z}} S_{l-m} B_m \\
& + \sum_{p\in\mathbb{Z}} \left(F_{1p}^- e^{-\mathrm{i}k_{2p}^1 x_2} + F_{1p}^+ e^{\mathrm{i}k_{2p}^1 x_2}\right) e^{\mathrm{i}k_{1p} x_1} \\
& - \sum_{p\in\mathbb{Z}}\sum_{l\in\mathbb{Z}} B_l \frac{e^{\mathrm{i}k_{2p}^1 L}\left(\alpha_p^0 - \alpha_p^1\right)^2}{D_p} \left(K_{pl}^+ e^{\mathrm{i}\left(k_{1p} x_1 + k_{2p}^1 x_2\right)} + K_{pl}^- e^{\mathrm{i}\left(k_{1p} x_1 - k_{2p}^1 x_2\right)}\right) \\
& + \sum_{p\in\mathbb{Z}}\sum_{l\in\mathbb{Z}} B_l \frac{\left(\left(\alpha_p^0\right)^2 - \left(\alpha_p^1\right)^2\right)}{D_p} \\
& \times \left(K_{pl}^+ e^{\mathrm{i}k_{2p}^1(a+b)} e^{\mathrm{i}\left(k_{1p} x_1 - k_{2p}^1 x_2\right)} + K_{pl}^- e^{-\mathrm{i}k_{2p}^1(a+b)} e^{\mathrm{i}\left(k_{1p} x_1 + k_{2p}^1 x_2\right)}\right) , \quad (44)
\end{aligned}
$$

wherein

$$
\begin{aligned}
D_p &= 2\mathrm{i}\sin\left(k_{2p}^1 L\right)\left(\left(\alpha_p^0\right)^2 + \left(\alpha_p^1\right)^2\right) - 4\alpha_p^0\alpha_p^1\cos\left(k_{2p}^1 L\right) , \\
F_{1p}^- &= -\frac{2\alpha_p^0\left(\alpha_p^0 + \alpha_p^1\right)}{D_p} e^{\mathrm{i}k_{2p}^1 b}\delta_{p0} , \\
F_{1p}^+ &= \frac{2\alpha_p^0\left(\alpha_p^0 - \alpha_p^1\right)}{D_p} e^{-\mathrm{i}k_{2p}^1 b}\delta_{p0} .
\end{aligned}
\quad (45)
$$

To proceed further, we need to convert the cartesian form to the cylindrical harmonic form:

$$
\begin{aligned}
p^1(\mathbf{r}) = {}& \sum_{l\in\mathbb{Z}} B_l H_l^{(1)}\left(k^1 r\right) e^{\mathrm{i}l\theta} + \sum_{l\in\mathbb{Z}} J_l\left(k^1 r\right) e^{\mathrm{i}l\theta} \sum_{m\in\mathbb{Z}} S_{l-m} B_m \\
& + \sum_{l\in\mathbb{Z}}\sum_{p\in\mathbb{Z}} \left(J_{lp}^- F_{1p}^- + J_{lp}^+ F_{1p}^+\right) J_l(k^1 r) e^{\mathrm{i}l\theta} \\
& \qquad\qquad\qquad + \sum_{l\in\mathbb{Z}} J_l\left(k^1 r\right) e^{\mathrm{i}l\theta} \sum_{n\in\mathbb{Z}}\sum_{p\in\mathbb{Z}} \left(Q_{lnp} - P_{lnp}\right) B_n , \quad (46)
\end{aligned}
$$

wherein

$$
\begin{aligned}
Q_{lnp} &= \frac{\left(\alpha_p^0\right)^2 - \left(\alpha_p^1\right)^2}{k_{2p}^1 D_p} \times \frac{4(-\mathrm{i})^{l-n}}{d}\cos\left(k_{2p}^1\left(a+b\right) + (l+n)\theta_p\right) , \\
P_{lnp} &= \frac{e^{\mathrm{i}k_{2p}^1 L}\left(\alpha_p^0 - \alpha_p^1\right)^2}{k_{2p}^1 D_p} \times \frac{4(-\mathrm{i})^{l-n}}{d}\cos\left((l-n)\theta_p\right) .
\end{aligned}
\quad (47)
$$

Central to the multipole method are the local field expansions or multipole expansions around each inclusion [4, 11, 29]. Because $p^1(\mathbf{r})$ satisfies a Helmholtz equation inside and outside the cylinder of the unit cell, in the vicinity of the cylinder we can write

$$
p^1(\mathbf{r}) = \sum_{l\in\mathbb{Z}} B_l H_l^{(1)}\left(k^1 r\right) e^{\mathrm{i}l\theta} + \sum_{l\in\mathbb{Z}} J_l\left(k^1 r\right) e^{\mathrm{i}l\theta} A_l . \quad (48)
$$

9

By identifying (46) with (48), we find

$$A_l = \sum_{m \in \mathbb{Z}} S_{l-m} B_m + \sum_{p \in \mathbb{Z}} \left(J_{lp}^- F_{1p}^- + J_{lp}^+ F_{1p}^+ \right) + \sum_{m \in \mathbb{Z}} \sum_{p \in \mathbb{Z}} (Q_{lmp} - P_{lmp}) B_m \ . \qquad (49)$$

At this point, we account for the two equations (12) and (13). It is well-known that the coefficients of the scattered field and those of the locally incident field are linked by a matrix relation depending on the parameters of the cylinder only, i.e.,

$$B_l = \frac{\gamma^1 \dot{J}_l(k^1 R) J_l(k^2 R) - \gamma^2 \dot{J}_l(k^2 R) J_l(k^1 R)}{\gamma^2 \dot{J}_l(k^2 R) H_l^{(1)}(k^1 R) - \gamma^1 \dot{H}_l^{(1)}(k^1 R) J_l(k^2 R)} A_l = R_l A_l \ , \qquad (50)$$

wherein $\gamma^j = \dfrac{k^j}{\rho^j}$. Denoting $\mathbf{B}$ the infinite column matrix of components B_l, (49) together with (50) may be written in the matrix form

$$(\mathbf{I} - \mathbf{R}\mathbf{S} - \mathbf{R}\,(\mathbf{Q} - \mathbf{P}))\,\mathbf{B} = \mathbf{R}\mathbf{F} \ . \qquad (51)$$

with $\mathbf{F}$ the column matrix of mth element $\sum\limits_{p \in \mathbb{Z}} J_{mp}^- F_{1p}^- + J_{mp}^+ F_{1p}^+$, $\mathbf{I}$ the identity matrix, $\mathbf{R}$ the diagonal matrix of component R_l and $\mathbf{S}$, $\mathbf{Q}$ and $\mathbf{P}$ three square matrices of respective (m, q)th element S_{m-q}, $\sum\limits_{p \in \mathbb{Z}} Q_{mqp}$ and $\sum\limits_{p \in \mathbb{Z}} P_{mqp}$.

Remark: In case of a Neumann type boundary condition, the relation (50) takes the form

$$B_l = \frac{-\dot{J}_l(k^1 R)}{\dot{H}_l^{(1)}(k^1 R)} A_l := R_l^{\mathcal{N}} A_l \ . \qquad (52)$$

8 Evaluation of the transmitted and reflected fields

Once (51) is solved for B_l, $\forall l \in \mathbb{Z}$, we can derive, from (37) and (41), expressions for R_p and T_p depending on B_l, $\forall l \in \mathbb{Z}$, which, after introduction into (15), leads to the expression of the pressure field in Ω_{0+}:

$$
\begin{aligned}
p^{0^+}(\mathbf{x}) = {}& e^{\mathrm{i}\left(k_1^i x_1 - k_2^{0i}(x_2 - a)\right)} + \frac{\mathrm{i}\sin\left(k_2^{1i} L\right)\left((\alpha^{0i})^2 - (\alpha^{1i})^2\right) e^{\mathrm{i}\left(k_1^i x_1 + k_2^{0i}(x_2 - a)\right)}}{\mathrm{i}\left((\alpha^{0i})^2 + (\alpha^{1i})^2\right)\sin\left(k_2^{1i} L\right) - 2\alpha^{1i}\alpha^{0i}\cos\left(k_2^{1i} L\right)} \\
& + \sum_{p \in \mathbb{Z}} \sum_{l \in \mathbb{Z}} \frac{4(-\mathrm{i}^l)}{dk_{2p}^1} \frac{1}{\mathrm{i}\left((\alpha_p^0)^2 + (\alpha_p^1)^2\right)\sin\left(k_{2p}^1 L\right) - 2\alpha_p^1 \alpha_p^0 \cos\left(k_{2p}^1 L\right)} \\
& \times \alpha_p^1\left(-\mathrm{i}\alpha_p^0 \sin\left(l\theta_p + k_{2p}^1 b\right) - \alpha_p^1 \cos\left(l\theta_p + k_{2p}^1 b\right)\right) e^{\mathrm{i}\left(k_{1p} x_1 + k_{2p}^0(x_2 - a)\right)} \ , \qquad (53)
\end{aligned}
$$

and, after introduction into (16), leads to

10

$$p^{0^-}(\mathbf{x}) = \frac{-2\alpha^{1i}\alpha^{0i}e^{\mathrm{i}\left(k_1^i x_1 - k_2^{0i}(x_2-b)\right)}}{\mathrm{i}\left((\alpha^{0i})^2 + (\alpha^{1i})^2\right)\sin\left(k_2^{1i}L\right) - 2\alpha^{1i}\alpha^{0i}\cos\left(k_2^{1i}L\right)}$$

$$+ \sum_{p\in\mathbb{Z}}\sum_{l\in\mathbb{Z}} \frac{4(-\mathrm{i}^l)}{dk_{2p}^1} \frac{1}{\mathrm{i}\left((\alpha_p^0)^2 + (\alpha_p^1)^2\right)\sin\left(k_{2p}^1 L\right) - 2\alpha_p^1\alpha_p^0\cos\left(k_{2p}^1 L\right)}$$

$$\times \alpha_p^1\left(\mathrm{i}\alpha_p^0\sin\left(l\theta_p + k_{2p}^1 a\right) - \alpha_p^1\cos\left(l\theta_p + k_{2p}^1 a\right)\right)e^{\mathrm{i}\left(k_{1p}x_1 - k_{2p}^0(x_2-b)\right)} . \quad (54)$$

9 Evaluation of pressure field in the slab

We obtain from (44) the final expression of the field in Ω_1:

$$p^1(\mathbf{x}) = \frac{2\alpha^{0i}\left(\mathrm{i}\alpha^{0i}\sin\left(k_2^{1i}(x_2-b)\right) - \alpha^{1i}\cos\left(k_2^{1i}(x_2-b)\right)\right)}{\mathrm{i}\left((\alpha^{0i})^2 + (\alpha^{1i})^2\right)\sin\left(k_2^{1i}L\right) - 2\alpha^{1i}\alpha^{0i}\cos\left(k_2^{1i}L\right)}$$

$$+ \sum_{l\in\mathbb{Z}} B_l H_l^{(1)}\left(k^1 r\right)e^{\mathrm{i}l\theta} + \sum_{l\in\mathbb{Z}} J_l\left(k^1 r\right)e^{\mathrm{i}l\theta}\sum_{m\in\mathbb{Z}} S_{l-m}B_m$$

$$- \sum_{p\in\mathbb{Z}}\sum_{l\in\mathbb{Z}} B_l \frac{2(-\mathrm{i}^l)}{dk_{2p}^1}\frac{1}{\mathrm{i}\left((\alpha_p^0)^2 + (\alpha_p^1)^2\right)\sin\left(k_{2p}^1 L\right) - 2\alpha_p^1\alpha_p^0\cos\left(k_{2p}^1 L\right)}$$

$$\times \cos(k_{2p}^1 x_2 + l\theta_p)e^{\mathrm{i}k_{2p}^1 L}\left(\alpha_p^0 - \alpha_p^1\right)^2 + \left((\alpha_p^1)^2 - (\alpha_p^0)^2\right)\cos(k_{2p}^1\left(x_2 - (a+b)\right) - l\theta_p) . \quad (55)$$

Use of the continuity conditions on Γ leads to:

$$p^2(\mathbf{r}) = \sum_{l\in\mathbb{Z}} \frac{\gamma^2 \dot{J}_l\left(k^2 R\right)J_l\left(k^1 R\right) - \gamma^1 \dot{J}_l\left(k^1 R\right)J_l\left(k^2 R\right)}{\gamma^1\left(\dot{H}_l^{(1)}\left(k^1 R\right)J_l\left(k^1 R\right) - \dot{J}_l\left(k^1 R\right)H_l^{(1)}\left(k^1 R\right)\right)}B_l J_l\left(k^2 r\right)e^{\mathrm{i}l\theta} . \quad (56)$$

Remark : The fields in Ω_j, $j = 0^+$, 1, 0^- are the sum of i) the field in absence of the inclusions (whose expressions are the same as those in [12]) with ii) the field due to the presence of the inclusions.

Remark : The field due to the presence of the inclusions, when compared with the Green's function as calculated in [12] in the case of a line source located in the slab, takes the form of the field radiated by induced periodic sources. The latter do not add energy to the system, but rather entail a redistribution of the energy in the frequency range of the solicitation.

10 Modal analysis

10.1 Modal analysis without inclusions

In the absence of inclusions, the resolution of the problem reduces to:

$$\begin{bmatrix} \left(\alpha^{1i} - \alpha^{0i}\right) & -e^{-\mathrm{i}k_2^{0i}L}\left(\alpha^{1i} + \alpha^{0i}\right) \\ \left(\alpha^{1i} + \alpha^{0i}\right) & -e^{\mathrm{i}k_2^{0i}L}\left(\alpha^{1i} - \alpha^{0i}\right) \end{bmatrix} \begin{bmatrix} T \\ R \end{bmatrix} = \begin{bmatrix} e^{-\mathrm{i}k_2^{0i}L}\left(\alpha^{1i} - \alpha^{0i}\right) \\ e^{\mathrm{i}k_2^{0i}L}\left(\alpha^{1i} + \alpha^{0i}\right) \end{bmatrix} . \quad (57)$$

The natural frequencies modes of the configuration are obtained by turning off the excitation. The resulting matrix equation possesses a non-trivial solution only if the determinant of the matrix vanishes, i.e. :

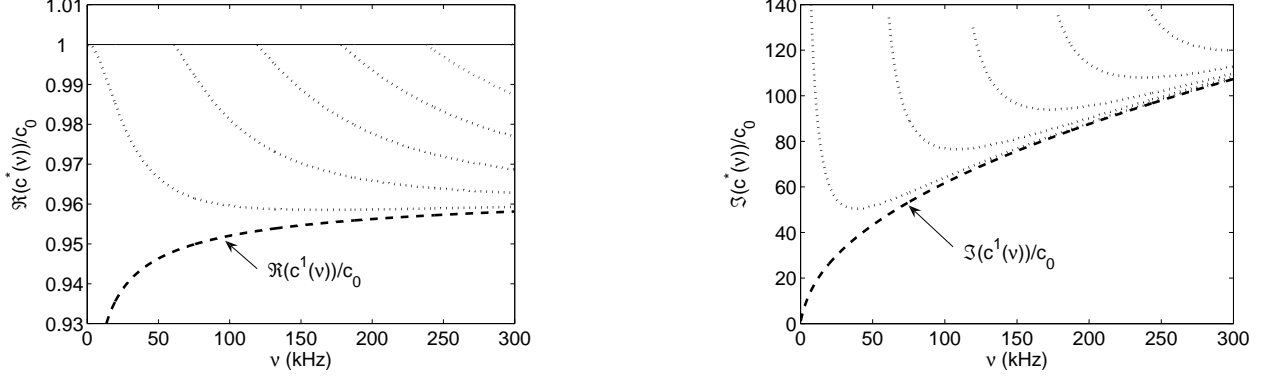$$\mathrm{i}\left((\alpha^{0i})^2 + (\alpha^{1i})^2\right)\sin\left(k_2^{1i}L\right) - 2\alpha^{1i}\alpha^{0i}\cos\left(k_2^{1i}L\right) = 0 \ . \tag{58}$$

Figure 2: Real part (left panel) and imaginary part (right panel) of the roots of the dispersion relation.

Fig. 2 depicts the real and the imaginary parts of the solution $c^\star(\omega) = \omega/(k_1^\star)$ of the previous equation with the mechanical characteristics used in the section 11. To solve the latter, we proceed as in [13]. The dispersion relation cannot vanish when the incident wave takes the form of a plane wave, because we must have $\Re\left(k_1^\star\right) \geq k^0$, whereas $k_1^i \in [-k_0, k_0]$ in case of a incident plane wave.

10.2   Modal analysis with inclusions

For the slab with periodic inclusions, the problem reduces to the resolution of the linear system (51). As previously, the natural frequencies of the modes of the configuration are obtained by turning off the excitation, embodied in the vector **RF**. The resulting equation possesses a non-trivial solution only if the determinant of the matrix vanishes:

$$\det\left(\mathbf{I} - \mathbf{RS} - \mathbf{R}\left(\mathbf{Q} - \mathbf{P}\right)\right) = 0 \ . \tag{59}$$

A procedure, called the partition method, for solving this equation, is not easy to apply because the off-diagonal elements of the matrix are not small compared to the diagonal elements. Even at low frequency (i.e. $\Re(k^1)R \ll 1$), $B_j = B_j^{(2)} \times \left(k^1 R\right)^2 + O\left(\left(k^1 R\right)^2\right)$ for $j = \{-1, 0, 1\}$, at least three terms should be taken into account.

An iterative scheme can be employed to solve (51) and obtain an approximate dispersion rela-

12

tion. We re-write this equation in the form

$$\left(1 - R_l \left(S_0 + \sum_{p \in \mathbb{Z}} (Q_{llp} - P_{llp})\right)\right) B_l =$$

$$R_l \sum_{m \in \mathbb{Z}} \left(S_{l-m} + \sum_{p \in \mathbb{Z}} (Q_{lmp} - P_{lmp})\right) B_m (1 - \delta_{ml})$$

$$+ R_l \sum_{p \in \mathbb{Z}} \left(J_{lp}^- F_{1p}^- + J_{lp}^+ F_{1p}^+\right), \forall l \in \mathbb{Z}. \quad (60)$$

The iterative procedure for solving this linear set of equations is:

$$\begin{cases} B_l^{(0)} = R_l \dfrac{\sum_{p \in \mathbb{Z}} \left(J_{lp}^- F_{1p}^- + J_{lp}^+ F_{1p}^+\right)}{1 - R_l \left(S_0 + \sum_{p \in \mathbb{Z}} (Q_{llp} - P_{llp})\right)} \\[2em] B_l^{(n)} = R_l \dfrac{1}{1 - R_l \left(S_0 + \sum_{p \in \mathbb{Z}} (Q_{llp} - P_{llp})\right)} \times \left[\sum_{p \in \mathbb{Z}} \left(J_{lp}^- F_{1p}^- + J_{lp}^+ F_{1p}^+\right) \right. \\[2em] \left. + \sum_{m \in \mathbb{Z}} \left(S_{l-m} + \sum_{p \in \mathbb{Z}} (Q_{lmp} - P_{lmp})\right) B_m^{(n-1)} (1 - \delta_{ml})\right], \forall n \in \mathbb{N}^*, \end{cases} \quad (61)$$

from which it becomes apparent that the solution of $B_l^{(n)}$, to any order of approximation, is expressed as a fraction, the denominator of which (not depending on the order of approximation), can become large for certain couples (k_{1p}, ω) so as to make $B_l^{(n)}$, and (possibly) the field large for these values.

When this happens, a natural mode of the configuration, comprising the inclusions and the slab, is excited, this taking the form of a resonance with respect to $B_l^{(n)}$, i.e. with respect to a plane wave component of the field in the slab relative to the inclusions. As $B_l^{(n)}$ is related to f_{1p}^+, f_{1p}^-, T_p and R_p, the structural resonance manifests itself for the same (k_{1p}, ω) as concerns the field in the slab and in the air.

$$1 - R_l \left(S_0 + \sum_{p \in \mathbb{Z}} (Q_{llp} - P_{llp})\right) = 1 - R_l \left(\sum_{j=1}^{\infty} H_0^{(1)} \left(k^1 jd\right) 2 \cos \left(k_1^i jd\right)\right.$$

$$+ \sum_{p \in \mathbb{Z}} \frac{2}{dk_{2p}^1} \frac{1}{\left(\mathrm{i} \sin \left(k_{2p}^1 L\right) \left(\left(\alpha_p^0\right)^2 + \left(\alpha_p^1\right)^2\right) - 2\alpha_p^0 \alpha_p^1 \cos \left(k_{2p}^1 L\right)\right)}$$

$$\left. \times \left(\cos \left(k_{2p}^1 (a+b) + 2l\theta_p\right) (-1)^l \left((\alpha_p^0)^2 - (\alpha_p^1)^2\right) - e^{\mathrm{i}k_{2p}^1 L} \left(\alpha_p^0 - \alpha_p^1\right)^2\right)\right) = 0. \quad (62)$$

13

The latter equation is the sum of a term linked to the grating embodied in $1 - R_l S_0$ with a term linked to the slab embodied in $-R_l \sum_{p \in \mathbb{Z}} (Q_{llp} - P_{llp})$. This can be interpreted as a perturbation of the dispersion relation of the gratings by the presence of the slab.

11 Numerical results

The ambiant and saturating fluid is the air medium ($\rho_0 = \rho_f = 1.213 kg.m^{-3}$, $c_0 = \sqrt{\frac{\gamma P_0}{\rho_0}}$, with $P_0 = 1.01325 \times 10^5 Pa$ and $\gamma = 1.4$, $\eta = 1.839 \times 10^{-5} kg.m^{-1}.s^{-1}$). The infinite layer is $1 \times 10^{-2} m$ thick and filled with a polymer foam M^1. The radius of the inclusions is constant equal to $R = 2.5 \times 10^{-3} m$. We vary the center-to-center distance between each inclusion from $d = 1 \times 10^{-2} m$ to $d = 2.5 \times 10^{-2} m$. The inclusions are either filled with the air medium (which define the so-called type 2 sample), with a melamin-foam (which define the so-called type 1 sample) or with such a material that the condition upon Γ is the Neumann one (which define the so-called type 3 sample).

The medium M^1 is characterized by $\phi = 0.96$, $\alpha_\infty = 1.07$, $\Lambda = 273 \times 10^{-6} m$, $\Lambda' = 672 \times 10^{-6} m$, $\sigma = 2843 N.s.m^{-4}$, while the melamine-foam is characterized by $\phi = 0.99$, $\alpha_\infty = 1.001$, $\Lambda = 150 \times 10^{-6} m$, $\Lambda' = 150 \times 10^{-6} m$, $\sigma = 12 \times 10^3 N.s.m^{-4}$. The incident angle is $\theta^i = 0$.

The infinite sum $\sum_{m \in \mathbb{Z}}$ over the indices of the modal representation of the diffracted field by a cylinder is truncated as $\sum_{m=-M}^{M}$ such that

$$M = \text{int}\left(\Re\left(4.05 \times \left(k^1 R\right)^{\frac{1}{3}} + k^1 R\right)\right) + 10 . \tag{63}$$

On the other hand, the infinite sum $\sum_{p \in \mathbb{Z}}$ over the indices of the k_{1p} is found to depend on the frequency and on the period of the grating. We also use an empirical rule we have determined by performing a large number of numerical experiments $\sum_{p=-P}^{P}$ such that

$$P = \frac{d\Re\left(k^1\right)}{2\pi} + 50\text{int}\left(e^{\frac{-\omega}{2\pi 50 \times 10^3}}\right) + 10\left(-\ln\left(\frac{d}{25 \times 10^{-3}}\right)\right) + 5 . \tag{64}$$

In the latter equations $\text{int}(a)$ represents the integer part of a.

The developed form of the conservation of energy relation takes the form of

$$1 = \mathcal{A} + \mathcal{R} + \mathcal{T} , \tag{65}$$

with $\mathcal{A}$, $\mathcal{R}$ and $\mathcal{T}$ the absorption, hemispherical reflection and hemispherical transmission coeffi-

cients respectively, defined by

$$\mathcal{R} = \sum_{p \in \mathbb{Z}} \frac{\Re\left(k_{2p}^0\right)}{k_2^{0i}} \|R_p(\omega)\|^2 = \sum_{p=-\bar{p}}^{\bar{p}} \frac{k_{2p}^0}{k_2^{0i}} \|R_p(\omega)\|^2 \ ,$$

$$\mathcal{T} = \sum_{p \in \mathbb{Z}} \frac{\Re\left(k_{2p}^0\right)}{k_2^{0i}} \|T_p(\omega)\|^2 = \sum_{p=-\bar{p}}^{\bar{p}} \frac{k_{2p}^0}{k_2^{0i}} \|T_p(\omega)\|^2 \ ,$$

(66)

wherein $\bar{p}$ is such that $\left(k_1^i + \dfrac{2\pi\left(\bar{p}+1\right)}{d}\right)^2 > (k^0)^2 \geq \left(k_1^i + \dfrac{2\pi\bar{p}}{d}\right)^2$.
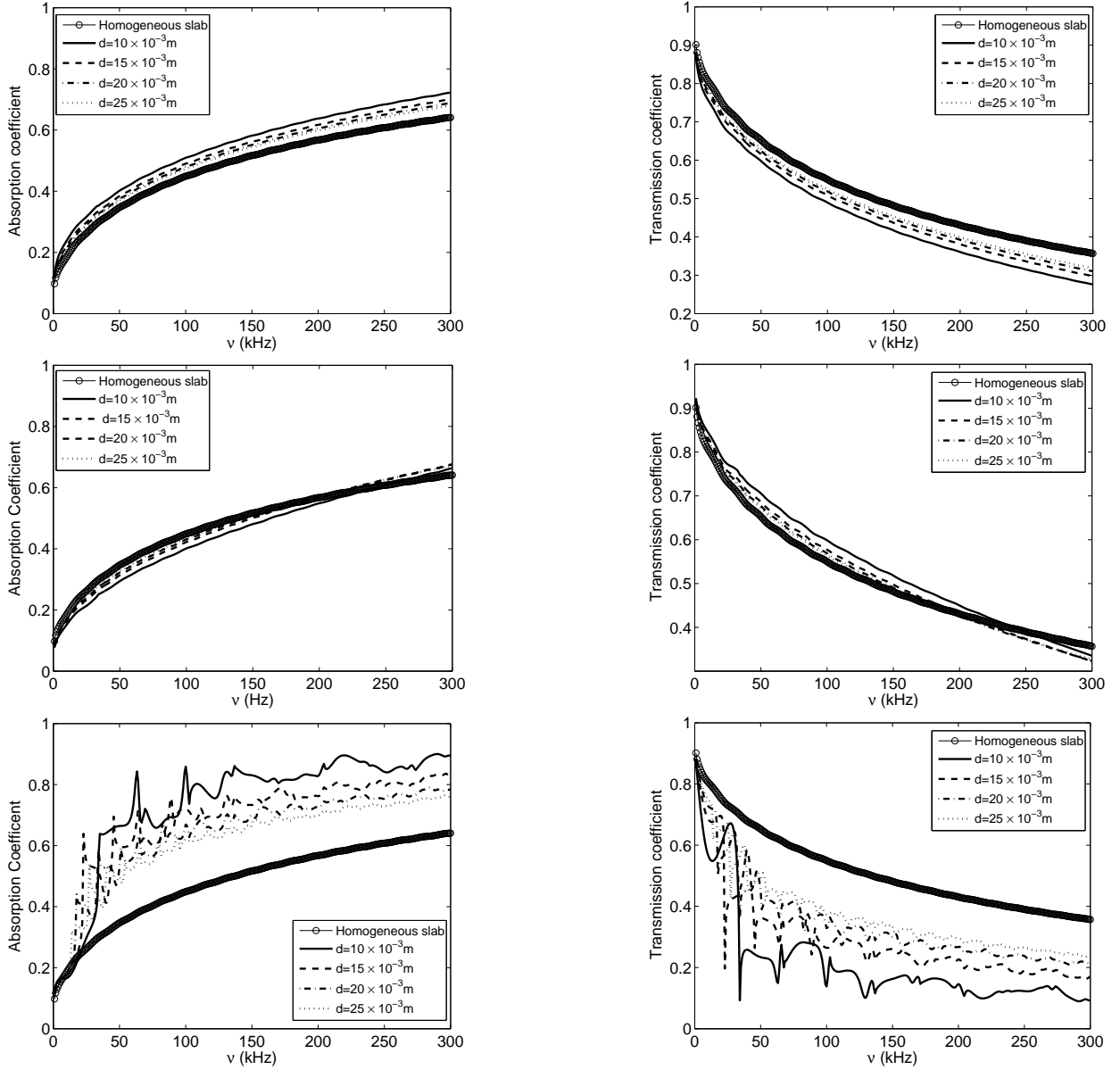
Figure 3: Comparison of the absorption (left panel) and hemispherical transmission (right panel) coefficients between the cases of inclusions of type referenced by 1 (top panels), 2 (middle panels) or 3 (bottom panels) for various center-to center distances.

The reflection coefficients are almost the same when compared with those as calculated in absence of inclusions except for closed inclusions of type 3. The increase of the absorption coefficient is also due to the decrease of the transmission coefficient, as was previously noticed in [27]. In all the cases, the larger is the spatial period, the closer the coefficients are to those of the case of a homogeneous slab.
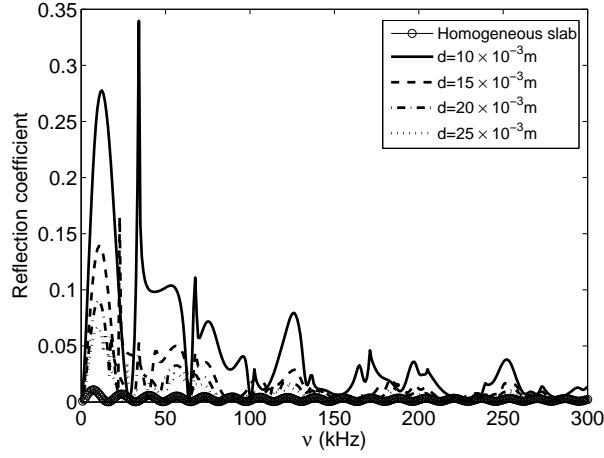
Figure 4: Comparison of the reflection coefficient with inclusions of type 3 for various center-to center distance.

Fig. 5 compares the reflection, transmission and absorption coefficients for $R = 2.5 \times 10^{-3} m$ and $R = 1 \times 10^{-3} m$ type 3 inclusions when $d = 10 \times 10^{-3} m$. The smaller the inclusions are, the closer the coefficients are to those of the case of the homogeneous slab.
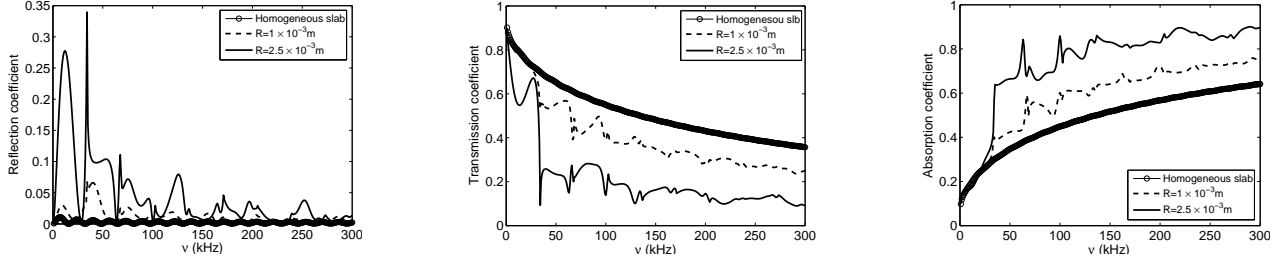

Figure 5: Comparison of the reflection, transmission and absorption coefficients for $R = 2.5 \times 10^{-3} m$ and $R = 1 \times 10^{-3} m$ type 3 inclusions when $d = 10 \times 10^{-3} m$.

12   Discussion

The addition of weak contrast inclusions (i.e. type 1 and type 2) leads to an absorption spectrum whose shape is close to that of a macroscopically-homogeneous slab. We also deal with an effective homogeneous porous slab, whose absorption coefficient is lower when the inclusions are filled with the air medium and larger when the inclusions are filled with an other, more absorptive, fluid-like porous medium. For fluid-like porous inclusions, the slope of the absorption coefficient is nearly the same as it is for the macroscopically-homogeneous slab, while for air inclusions (holes) the slope is larger. That is why at low frequency the absorption coefficient is lower than the one as calculated for the homogeneous slab and becomes larger for a higher frequency.

The addition of high-contrast inclusions (i.e. type 3) leads to an absorption spectrum that is, on the average, larger than for the macroscopically-homogeneous slab, and which presents some additional peaks. The slope of the absorption spectrum is closer to that of the the macroscopically-homogeneous slab. Each peak leads to a supplementary increase of the absorption of the configu-

ration. The absorption can be multiplied by a factor of three at the location of some of these peaks when compared with the one of the macroscopically-homogeneous slab. Two types of peaks are distinguished. Each of them appears periodically for a specific period of the inclusions and can be associated with mode excitation of the whole configuration.

Two peaks stand out for all center-to-center distances at the same frequencies near $\nu = 65kHz$, $\nu = 133kHz$. This corresponds to the excitation of quasi-mode 2 and 3 of the initial slab . A quasi-mode is a mode of the global configuration whose structure is close to the one of a mode of a sub-structure it is composed of. Quasi-mode 1 occurs for a frequency too low for it to be seen, and quasi-mode 3 is largely attenuated. The excitation of the quasi-mode of the slab is made possible by the spatial periodicity of the configuration.

In the absence of the inclusions, the modes of a homogeneous slab filled with a fluid-like porous medium cannot be excited by an incident plane wave propagating in the air [15]. If $det(\mathbf{E}) = 0$ denotes a generic dispersion relation, then we can say that $det(\mathbf{E})$ is close to zero (vanishes in absence of dissipation) only for an evanescent wave in the air medium, which cannot be excited by an incident plane bulk wave.

The spatially-periodic configuration leads to a field representation, through the Floquet theorem, that includes evanescent waves the air medium. Another explanation of the quasi-mode excitation relies on the fact that each inclusion acts as an induced cylindrical source. The response of an active cylindrical source radiating in the neighborhood of a homogeneous slab (see [12]) enables a mode of this slab to be excited because some of the waves radiated by the source are evanescent and have the same structure (at resonance) as that of the evanescent wave associated with the mode.

The other peaks appear in a periodic manner beyond the peak relative to the quasi-mode of the slab. Their periodicity is inversely proportional to the spatial periodicity d of the grating. This phenomena was already encountered in [14] and was attributed to a periodization of the quasi-mode due to the primitive reciprocal lattice vector $\mathbf{k_1} = \dfrac{2\pi}{d}\mathbf{i_1}$. This periodization is strongly associated with the excitation of quasi Cutler-modes.

The increase of the absorption is also due to an average (global) increase which does not take the form of additional peaks. This global increase can be explained by multipathing between each inclusion and/or by excitation of evanescent waves in the slab, thanks to the existence of the grating.

Addition of high contrast inclusions also leads to an increase of the absorption of the slab, largely associated with a decrease of the transmission coefficient. This is mainly due to mode excitation of the whole configuration, whose structure consists of evanescent waves in the air medium (and in the slab), thus leading to an entrapment of the energy in the slab. The latter is dissipated by thermal and viscous effects.

In all the cases, the closer the inclusions are, and/or the larger are their radii, the larger is the absorption.

13 Conclusion

We show that high-contrast, periodically-arranged, inclusions in a porous slab induce an increase of the absorption coefficient, mainly associated with a decrease of the transmission coefficient over a large frequency range, and in particular, at low frequencies (although higher than $\sim 20kHz$). This effect is due to mode excitation of the slab through excitation of the quasi-mode of the initial slab

(enabled) by the periodic inclusions, and to excitation of grating modes via multipathing between the inclusions.

This increase of absorption is most noticeable for rigid frame porous inclusions in a large portion of the frequency range, and is less pronounced for air inclusions.

The reflection coefficients are found to be of the same order as those in the absence of inclusions for low-contrast inclusions, and to be higher than those in the absence of inclusions for high contrast inclusions. The way of reducing the reflection is by acting on the surface geometry of the slab. A first approach can consist in the addition of a homogenized layer of double porosity [24].

Acknowledgment

A   Numerical validation

We validate the numerical implementation of the analytical calculation with the help of our Finite-Element code [16], in the case of a viscoacoustic medium (Fig. 6).

The medium filling Ω_0 is the air medium ($\rho_0 = \rho_f$, $c_0 = \sqrt{\dfrac{\gamma P_0}{\rho_0}}$). The infinite slab and the inclusion are filled with viscoacoustic media whose relaxed characteristics are those of the porous medium when the dissipative aspects vanish, (i.e. $\rho_1 = \dfrac{c_0 \times 0.96}{1.07}$, $c_1 = \dfrac{c_0}{\sqrt{1.07}}$ and $\rho_2 = \dfrac{\rho_0 \times 0.99}{1.001}$, $c_2 = \dfrac{c_0}{\sqrt{1.001}}$). The dissipative aspects of M^1 and M^2 are described by constant quality factors over the frequency range of solicitation, such that $Q^1 = 30$ and $Q^1 = 50$.

The numerical simulations are performed on a grid of 3000×400 nodes, whose grid spacing is equal to $1 \times 10^{-4}m$. The slab is $2 \times 10^{-2}m$ thick and the center-to-center distance between two adjacent cylinders is $1.5 \times 10^{-2}m$. The radius of each cylinder is $R = 5 \times 10^{-3}m$.

The signal spectrum of the solicitation is that of a Ricker pulse centered at $\nu_0 = 100kHz$. The incident angle is $\theta^i = 0$.
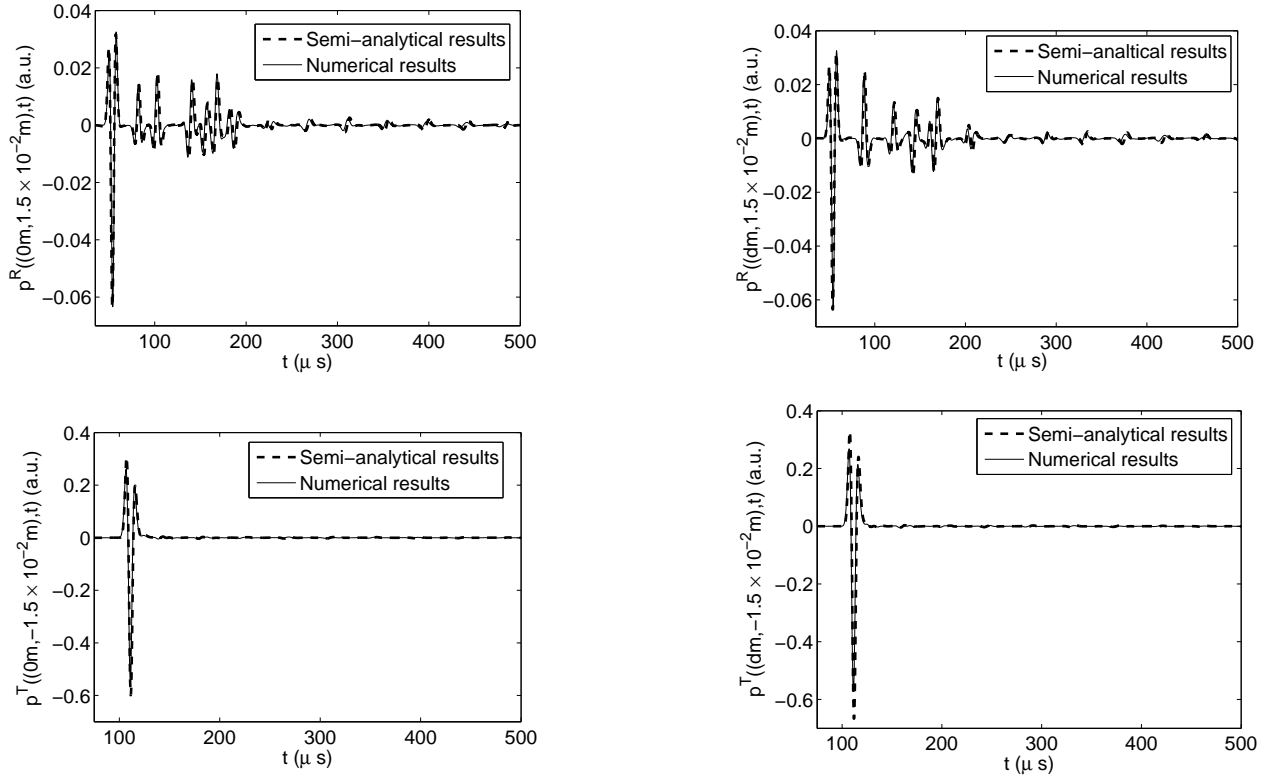
Figure 6: Comparison between the reflected and transmitted pressure field as calculated by the semi-analytical method and as calculated by the FE code. The top panels depict the reflected field, while the bottom panels depict the transmitted field for both a central location (left panels) and appendicular location (right panels) of the unit cells.

References

[1] M. Abramovitz and I. Stegun. *Handbook of Mathematical Functions.* Dover, New-York, 1970.

[2] J.-F. Allard and Y. Champoux. New empirical equations for sound propagation in rigid frame porous materials. *J. Acoust. Soc. Am.*, 91:3346–3353, 1992.

[3] P.-Y. Bard and A. Wirgin. Effects of buildings on the duration and amplitude of ground motion in mexico city. *Bull. Seism. Soc. Am.*, 86:914–920, 1996.

[4] L.C. Botten, N.A.P. Nicorovici, A.A. Asatryan, R.C. McPhedran, C.G. Poulton, C.M. de Sterke, and P. Robinson. Formulation for electromagnetic scattering and propagation through grating stacks of metallic and dielectric cylinders for photonic crystal calculations. parti method. *J. Opt. Soc. Am. A*, 17:2165–2176, 2005.

[5] C. Boutin, P. Royer, and J.-L. Auriault. Acoustic absorption of porous surfacing with dual porosity. *Int. J. Solids Struct.*, 35:4709–4737, 1998.

[6] B. Budiansky. On the elastic moduli of some heterogeneous materials. *J. Mech. Phys. Solids*, 13:223–227, 1965.

[7] Cutler C.C. Technical Report MM 44-160-218, Bell Telephone Lab, 1944.

[8] J.J. Cuomo, J.F. Ziegler, and J.M. Woodhall. A new concept for solar energy thermal conversion. *Appl. Phys. Let.*, 26:557–559, 1992.

[9] A. de Bruijn. Anomalous effects in the sound absorption of periodically uneven surfaces. *Acustica*, 24:75–84, 1971.

[10] L. De Ryck, J.P. Groby, Ph. Leclaire, W. Lauriks, A. Wirgin, C. Depollier, and Z.E.A. Fellah. Acoustic wave propagation in a macroscopically inhomogeneous porous medium saturated by a fluid. *Appl. Phys. Lett.*, 90:181901, 2007.

[11] D. Felbacq, G. Tayeb, and D. Mayster. Scattering by a random set of parallel cylinders. *J. Opt. Soc. Am. A*, 11:2526–2538, 1994.

[12] J.-P. Groby, L. De Ryck, P. Leclaire, A. Wirgin, W. Lauriks, Gilbert R.P., and Y.S. Xu. Use of specific Green's functions for solving direct problems involving a heterogeneous rigid frame porous medium slab solicited by the acoustic waves. *Math. Meth. Appl. Sci.*, 30:91–122, 2007.

[13] J.-P. Groby and A. Wirgin. 2D ground motion at a soft viscoelastic layer/hard substratum site in response to SH cylindrical waves radiated by deep and shallow line sources: Numerical results. *Geophys. J. Intl.*, 163:192–224, 2005.

[14] J.-P. Groby and A. Wirgin. Seismic motion in urban sites consisting of blocks in welded contact with a soft layer overlying a hard half space. 2007. submitted to Geophys. J. Intl.

[15] J.P. Groby, E. Ogam, A. Wirgin, Z.E.A. Fellah, W. Lauriks, J.-Y. Chapelon, C. Depollier, L. De Ryck, R. Gilbert, N. Sebaa, and Y. Xu. 2D mode excitation in a porous slab saturated with air in the high frequency approximation. In *Symposium on the Acoustics of Poro-Elastic Materials*, pages 53–60, ENTPE, Lyon, France, December 2005.

[16] J.P. Groby and C. Tsogka. A time domain method for modeling viscoacoustic wave propagation. *J. Compt. Acoust.*, 14:201–236, 2006.

[17] Z. Hashin and S. Shtrikman. A variational approach to the theory of the elastic behaviour of multiphase materials. *J. Mech. Phys. Solids*, 11:127–140, 1963.

[18] C.M. Horwitz. Solar-selective globular metal films. *J. Opt. Soc. Am.*, 68:1032–1038, 1978.

[19] J.D. Joannopoulos, R.D. Meade, and J.N. Winn. *Photonic Crystals; Molding the Flow of Light*. Princeton University Press, Princeton, 1995.

[20] D.J. Johnson, J. Koplik, and Dashen R. Theory of dynamic permeability and tortuosity in fluid-saturated porous media. *J. Fluid Mech.*, 176:379–402, 1987.

[21] L. Kelders, J.-F. Allard, and W. Lauriks. Ultrasonic surface waves above rectangular-groove gratings. *J. Acoust. Soc. Am.*, 103(5):2730–2733, 1998.

21

[22] A. Khelif, B. Djafari-Rouhani, V. Laude, and M. Solal. Coupling characteristics of localized phonons in photonic crystal fibers. *J. Appl. Phys.*, 94(12):7944–7946, 2003.

[23] V. Laude, M. Wilm, S. Benchabane, and A. Khelif. Full band gap for surface acoustic waves in a piezoelectric phononic crystal. *Phys. Rev. E*, 71:036607, 2003.

[24] X. Olny and C. Boutin. Acoustic wave propagation in double porosity media. *J. Acoust. Soc. Am.*, 113:73–89, 2003.

[25] B. Sapoval, B. Hebert, and S. Russ. Experimental study of a fractal acoustical cavity. *J. Acoust. Soc. Am.*, 105:2014–2019, 1999.

[26] J.B Tanneau, O. amd Casimir and P. Lamary. Optimization of multilayered panels with poroelastic components for an acoustical transmission objective. *J. Acoust. Soc. Am.*, 120(3):1227–1238, 2006.

[27] V. Tournat, V. Pagneux, D. Lafarge, and L. Jaouen. Multiple scattering of acoustic waves and porous absorbing media. *Phys. Rev. E.*, 70:026609, 2004.

[28] V.G. Veselago. The electrodynamics of substances with simultaneous negative value of e and m. *Sov. Phys. Usp.*, 10:509–514, 1968.

[29] S. Wilcox, L.C. Botten, R.C. McPhedran, C.G. Poulton, and C.M. de Sterke. Modeling of defect modes in photonic crystals using the fictitious source superposition method. *Phys. Rev. E*, 71:056606, 2005.

[30] M. Wilm, K. Khelif, S. Ballandras, V. Laude, and B. Djafari-Rouhani. Out-of-plane propagation of elastic waves in two-dimensional phononic band-gap material. *Phys. Rev. E*, page 065602, 2003.

[31] R.W. Wood. A suspected case of the electrical resonance of minute metal particles for lightwaves. a new type of absorption. *Philosophical Magazine and Journal of Science*, 4:369, 1902.

[32] T.T. Wu. The effect of inclusion shape on the elastic moduli of the two-phase material. *Int. J. Solids Struct.*, 1:1–8, 1966.

[33] E. Yablonovitch. Photonic band-gap structures. *J. Opt. Soc. Am. B*, 10(2):283–295, 1993.